Supporting Information

Johnson et al. 10.1073/pnas.1207532109

SI Materials and Methods

Subject Statistics. ***Subject 1; 26-y-old female, focal cortical dysplasia, right frontal seizure focus.*** Functional screening was run on this subject on the third day following surgery. This screening revealed a spatially localized high-gamma response for overt and imagined tongue movement. No such response was observed for hand movement, suggesting that the grid did not provide any coverage of hand-motor cortex. On the next day the subject was introduced to a two-target brain–computer interface (BCI) task. Electrode 23 was initially chosen as the control electrode; however, the subject's control using this electrode was poor. The control signal was subsequently switched to electrode 24, at which point the subject's performance improved considerably. The subject did one set of 18 trials using electrode 23 on a two-target task with overt movement. The subject then did two sets of 18 trials using electrode 24 and overt movement. After this, the subject performed one set of 18 trials of the two-target BCI task using imagery. Six separate nonrapid eye movement (NREM) sleep epochs were identified on the pretraining night. Combined, these epochs comprised 2.83 h, which were broken down into 170 60-s sections. In the posttraining night, nine NREM sleep epochs were identified for a total of 4.8 h and 288 60-s sections. The minimum coincidence was 0.0029 on day 1 and 0.0024 on day 2; the maximum observed coincidence was 0.39 on both days. The average coincidences were 0.15 and 0.13 for days 1 and 2, respectively.

Subject 2; 18-y-old male, cavernoma, right frontal–parietal seizure focus. Functional screening was run on this subject on the third day following surgery. Due to a sizeable lesion, the subject showed significant reorganization of motor cortex. The screening revealed a spatially specific high-gamma response for overt and imagined hand movement at electrode 33. A similar response was observed for tongue movement on electrodes 44 and 60. However, the amplitude of the difference in high-gamma power between activity and rest was smaller than for hand movement. Later in the same day, the subject was introduced to a two-target BCI task using electrode 33 as the control electrode. The subject did 18 trials with a two-target task using overt movement and used imagery for all subsequent trials. In two recording sessions on the same evening, the subject performed one set of 18 trials on the two-target task, one set of 18 trials on the three-target task, two sets of 18 trials on the five-target task, and one set of 50 trials on the six-target task. During the pretraining night, two NREM sleep epochs were identified, totaling 1.6 h and 53 60-s sections. On the posttraining night, five NREM sleep epochs were identified, totaling 3.38 h and 203 60-s sections. The minimum coincidence was 0 and the maximum observed coincidence was 0.37 on day 1 and 0.25 on day 2. The average coincidences were 0.07 and 0.04 for days 1 and 2, respectively.

Subject 3; 17-y-old female, postcontusion, right frontal pole seizure focus. Presurgical functional MRI (fMRI) was used to identify motor and premotor regions; these locations were confirmed postoperatively with a functional screening task and electrical stimulation. In addition to a standard-sized grid, this subject was also implanted with a minigrid. Other electrodes were implanted frontally and interhemispherically, but are not included in this analysis. The subject was trained to control a two-target BCI with hand motor imagery. The control electrode, number 66 on the minigrid, was over premotor cortex. The control signal was based on the power in the beta band rather than the high-gamma band. Before controlling the cursor with imagery, the subject practiced the task using overt movement in one set of 29 trials. In one training session, the subject performed six sets of 29 imagery trials. On the pretraining night, eight different NREM sleep epochs were identified for a total of 2.87 h and 172 60-s sections. On the posttraining night, three different NREM sleep epochs were identified for a total of 1.98 h and 119 60-s sections. The minimum coincidence was 0 and the maximum observed coincidence was 0.34 on day 1 and 0.39 on day 2. The average coincidences were 0.21 and 0.27 for days 1 and 2, respectively.

Subject 4; 16-y-old female, tuberous sclerosis, left temporal seizure focus (control subject). In this subject, functional screening showed that several electrodes (6, 7, 14, and 15) responded to overt hand movement and two electrodes (21 and 28) responded to overt tongue movement. This subject participated in a different set of language-based experiments and was not trained on a BCI. The data presented in this study were taken from the third and fourth day after surgery. During the first night, four NREM sleep epochs were identified, totaling 2.5 h and 149 60-s sections. On the second night, three NREM sleep epochs were identified, totaling 3.51 h and 209 60-s sections. The minimum coincidence was 0 and the maximum observed coincidence was 0.50 on both days 1 and 2. The average coincidences were 0.036 and 0.044 for days 1 and 2, respectively.

Subject 5; 29-y-old male, ganglioglioma, right frontal seizure focus (control subject). In this subject functional screening showed that several electrodes (32, 40, and 46) responded to overt hand movement and two electrodes (45 and 54) responded to overt tongue movement. Although electrode 45 responded to tongue movement, its location on the postcentral gyrus suggests that it was over the sensory cortex. This subject was not trained on a BCI until the sixth day after surgery. The subject was not able to achieve better than chance performance on this task and did not participate in very many trials. The data presented in this study were taken from the third and fourth day after surgery before the subject was introduced to the task. During the first night, five NREM sleep epochs were identified, totaling 5.92 h and 356 60-s sections. On the second night, five NREM sleep epochs were identified, totaling 3.73 h and 222 60-s sections. The minimum coincidence was 0 and the maximum observed coincidence was 0.29 on day 1 and 0.28 on day 2. The average coincidences were 0.021 and 0.020 for days 1 and 2, respectively. In this subject, whereas most of the electrodes show a low level of coincidence, there are only four electrode pairs showing strongly coincident spindles. It is not clear why this is the case. Compared with the other subjects this subject's sleep had a higher level of background noise (spikes, oscillations at other frequencies, etc.) and some spindles may have been obscured by these events. It is also possible that the lack of coincidence is related to the subject's pathology.

Potential Confounds. These data were collected from epileptic patients who were not only tapering off of their antiseizure medication, but also taking pain medication. Patients slept in a noisy acute care hospital environment, had pain and movement restrictions, had noisy family members at bedside, were woken up for nursing care, and were sometimes told to stay up to precipitate seizures. Epilepsy and sleep have a known interaction, and medications may affect sleep patterns. Nir et al. (1) showed that sleep measures in a similar population were within the normal range, although their subjects had not yet started tapering off of their antiseizure medications. We opted to start our experiments later in the course of the subjects' clinical monitoring to minimize the confounding effect of anesthesia and i.v. narcotics.

The seizure foci for subjects included in this study were outside of the motor area, and the analyzed sleep data does not include any seizures, but interictal spikes were present to a varying degree in all subjects. To avoid misclassification of spikes as spindles all detected spikes had to exceed a periodicity requirement based on the autocorrelation.

In the absence of electrooculogram, electromyogram, video, and scalp electroencephalography, sleep stages could not be classified. NREM sleep epochs were identified based on delta power, which introduces a bias toward deeper stages of sleep when spindles are less prevalent. An increase in epileptic activity due to the tapering of antiepileptic medications could lead to more awakenings and thus more fragmented sleep and a bias toward earlier sleep stages. However, in our subject set, some subjects had more fragmented sleep on the second night, whereas some had less fragmented sleep on the second night, and thus this is not a consistent factor in our results.

Because of the nature of our subject population, subjects capable of performing cognitively challenging tasks such as BCI are rare, whereas at the same time the demand for experimental access to these high-functioning subjects is very high. Because BCI is a major focus of our research group, all subjects who are able to learn this task are trained every day that they are willing to train. Thus, unfortunately, we cannot provide within-subject controls.

1. Nir Y, et al. (2011) Regional slow waves and spindles in human sleep. *Neuron* 70(1): 153–169.

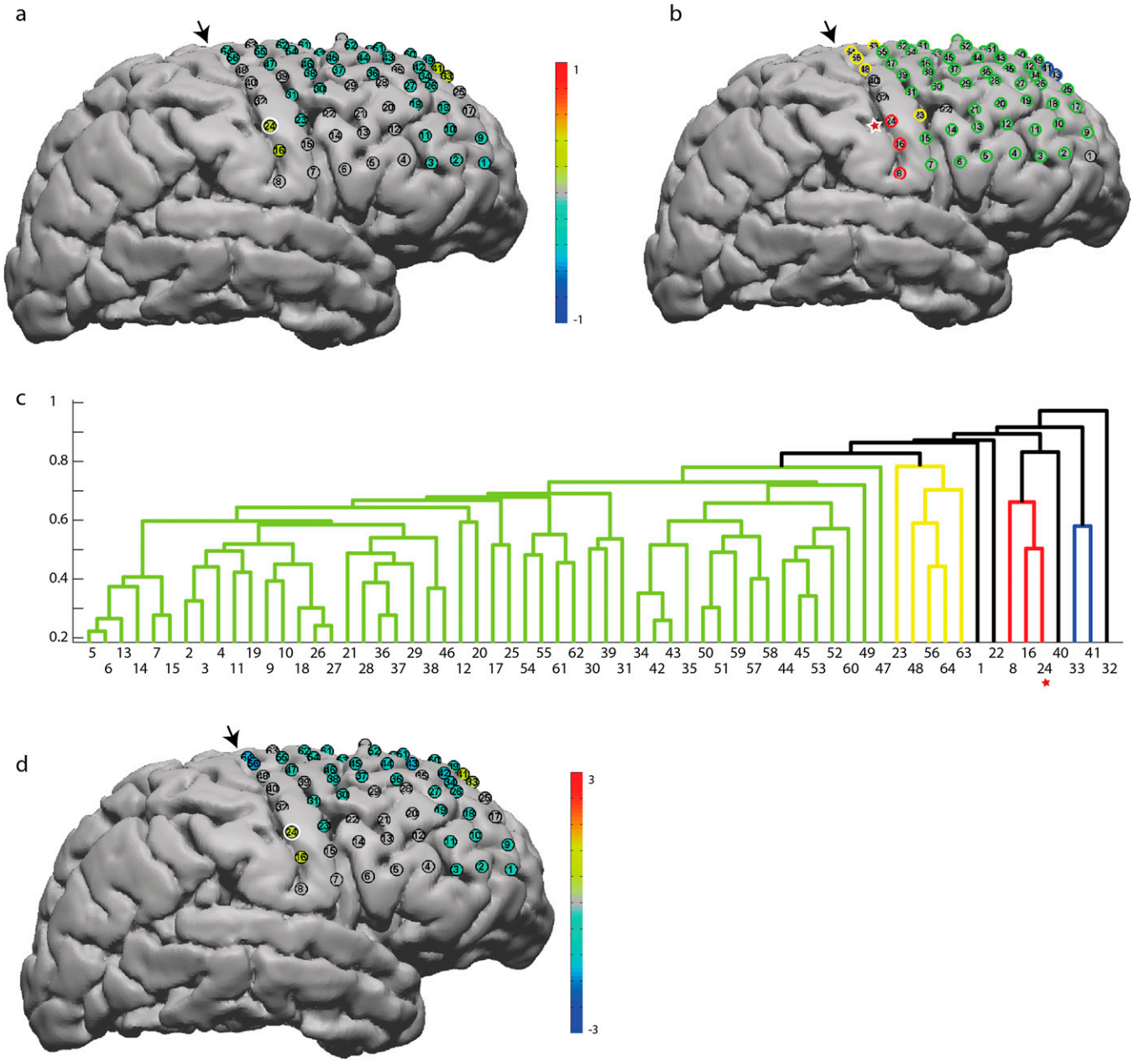

Fig. S1. Subject 1 results (trained). (*A*) For each electrode, the difference between the average rate of spindle occurrence in pre- and posttraining sleep is plotted on the subject's cortex as a ratio of the sum of the means. Warm colors indicate a rate increase; cool colors indicate a rate decrease. Electrodes that showed no significant ($P < 0.001$, Bonferroni corrected for multiple comparisons) change are drawn in gray. The electrode that was used for BCI control is circled in white. (*B*) Coincidence-based "distance" was used to cluster electrodes in spindle space. The dendrogram (*C*) shows the relative closeness of electrodes in this space. In this case, the dendrogram was created from posttraining sleep. The distance between electrodes, plotted on the *x* axis, has a maximum value of 1 and a minimum value of 0. Clusters are formed by setting a distance threshold; here a threshold of 85% of the maximum distance was used. Example clusters are shown in different colors in the dendrogram and plotted with the same colors on the cortex (*B*). The task electrode is marked with a star below the dendrogram. For comparison, a similar star has been placed just to the left of the task electrode on the corresponding cortical surface (*B*). (*D*) The absolute difference between the average rate of spindle occurrence in pre- and posttraining sleep is plotted on the subject's cortex. Warm colors indicate a rate increase; cool colors indicate a rate decrease. Electrodes that showed no significant ($P < 0.001$, Bonferroni corrected for multiple comparisons) change are drawn in gray. The electrode that was used for BCI control is circled in white. The central sulcus is marked with a black arrow in *A*–*D*.

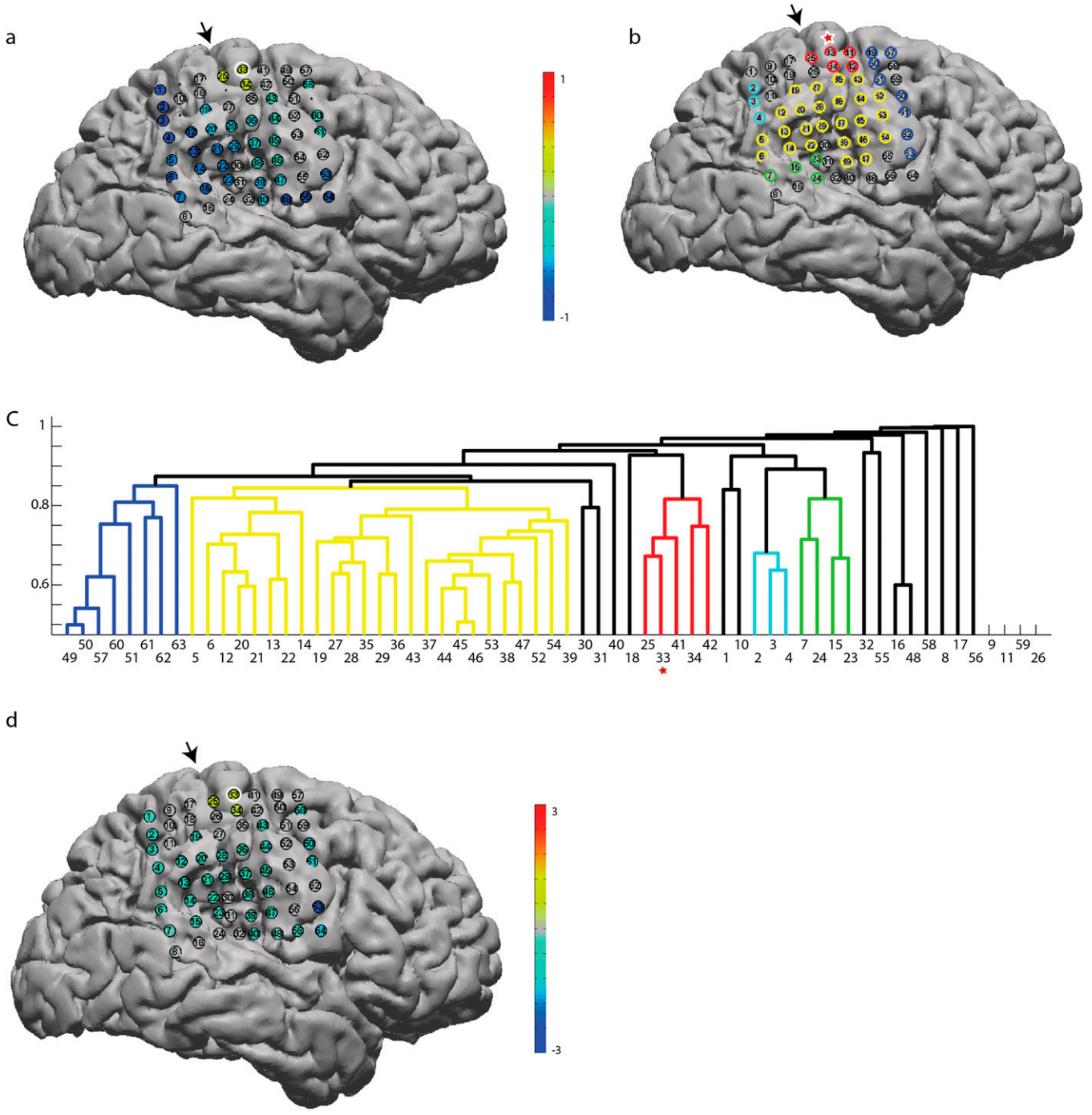

Fig. S2. Subject 2 results (trained). (*A*) For each electrode, the difference between the average rate of spindle occurrence in pre- and posttraining sleep is plotted on the subject's cortex as a ratio of the sum of the means. Warm colors indicate a rate increase; cool colors indicate a rate decrease. Electrodes that showed no significant ($P < 0.001$, Bonferroni corrected for multiple comparisons) change are drawn in gray. The electrode that was used for BCI control is circled in white. (*B*) Coincidence-based "distance" was used to cluster electrodes in spindle space. The dendrogram (*C*) shows the relative closeness of electrodes in this space. In this case, the dendrogram was created from posttraining sleep. The distance between electrodes, plotted on the *x* axis, has a maximum value of 1 and a minimum value of 0. Clusters are formed by setting a distance threshold; here a threshold of 85% of the maximum distance was used. Example clusters are shown in different colors in the dendrogram and plotted with the same colors on the cortex (*B*). The task electrode is marked with a star below the dendrogram. For comparison, a similar star has been placed just above the task electrode on the corresponding cortical surface (*B*). (*D*) The absolute difference between the average rate of spindle occurrence in pre- and post training sleep is plotted on the subject's cortex. Warm colors indicate a rate increase; cool colors indicate a rate decrease. Electrodes that showed no significant ($P < 0.001$, Bonferroni corrected for multiple comparisons) change are drawn in gray. The electrode that was used for BCI control is circled in white. The central sulcus is marked with a black arrow in *A*–*D*.

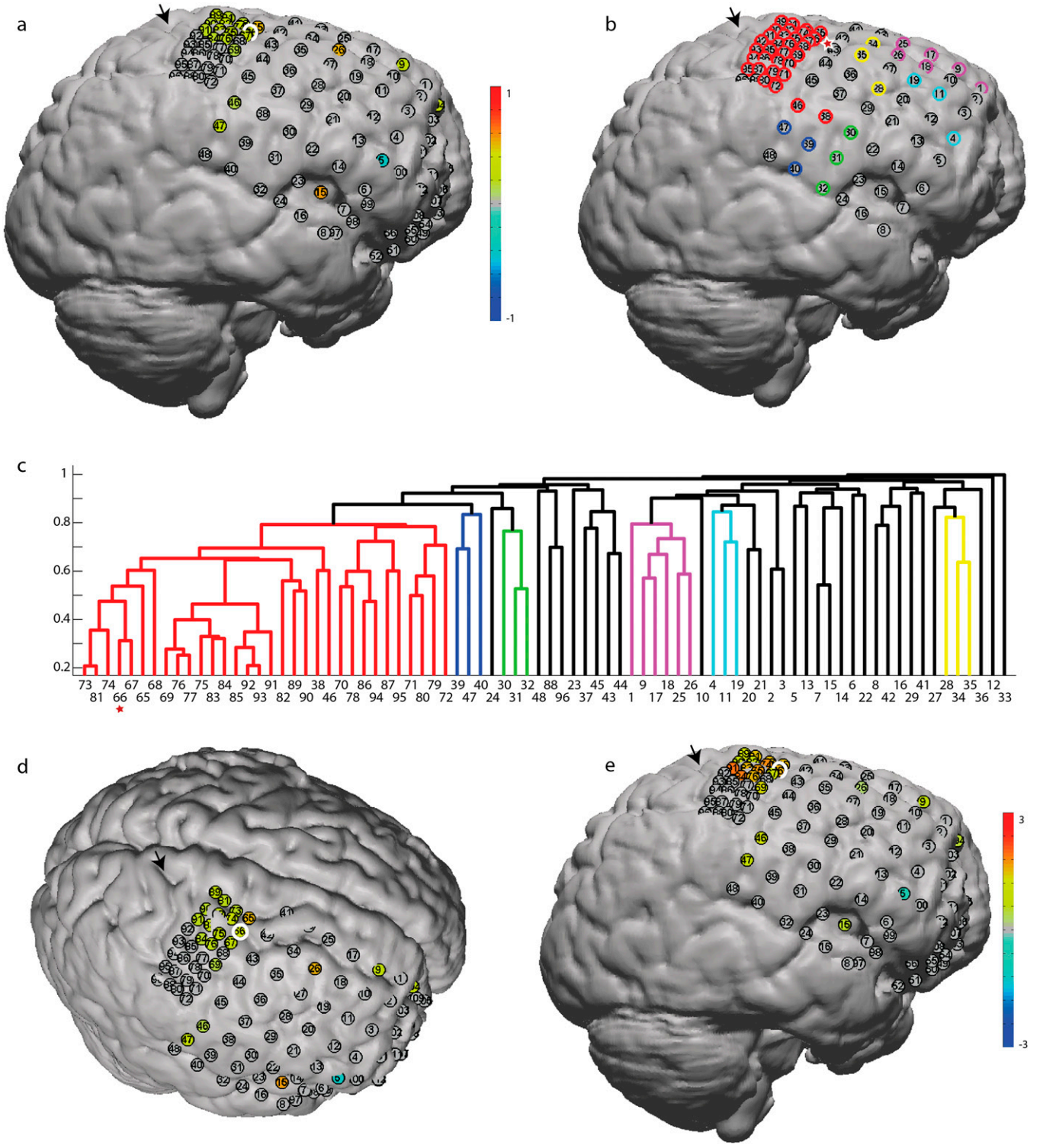

Fig. S3. Subject 3 results (trained). (*A*) For each electrode, the difference between the average rate of spindle occurrence in pre- and posttraining sleep is plotted on the subject's cortex as a ratio of the sum of the means. Warm colors indicate a rate increase; cool colors indicate a rate decrease. Electrodes that showed no significant ($P < 0.001$, Bonferroni corrected for multiple comparisons) change are drawn in gray. The electrode that was used for BCI control is circled in white. (*B*) Coincidence-based "distance" was used to cluster electrodes in spindle space. The dendrogram (*C*) shows the relative closeness of electrodes in this space. In this case, the dendrogram was created from posttraining sleep. The distance between electrodes, plotted on the *x* axis, has a maximum value of 1 and a minimum value of 0. Clusters are formed by setting a distance threshold; here a threshold of 85% of the maximum distance was used. Example clusters are shown in different colors in the dendrogram and plotted with the same colors on the cortex (*B*). The task electrode is marked with a star below the dendrogram. For comparison, a similar star has been placed just to the right of the task electrode on the corresponding cortical surface (*B*). Panel *D* is the same as panel *B*, except that the brain has been rotated to provide a better view of the task electrode. (*E*) The absolute difference between the average rate of spindle occurrence in pre- and posttraining sleep is plotted on the subject's cortex. Warm colors indicate a rate increase; cool colors indicate a rate decrease. Electrodes that showed no significant ($P < 0.001$, Bonferroni corrected for multiple comparisons) change are drawn in gray. The electrode that was used for BCI control is circled in white. The central sulcus is marked with a black arrow in *A*–*E*.

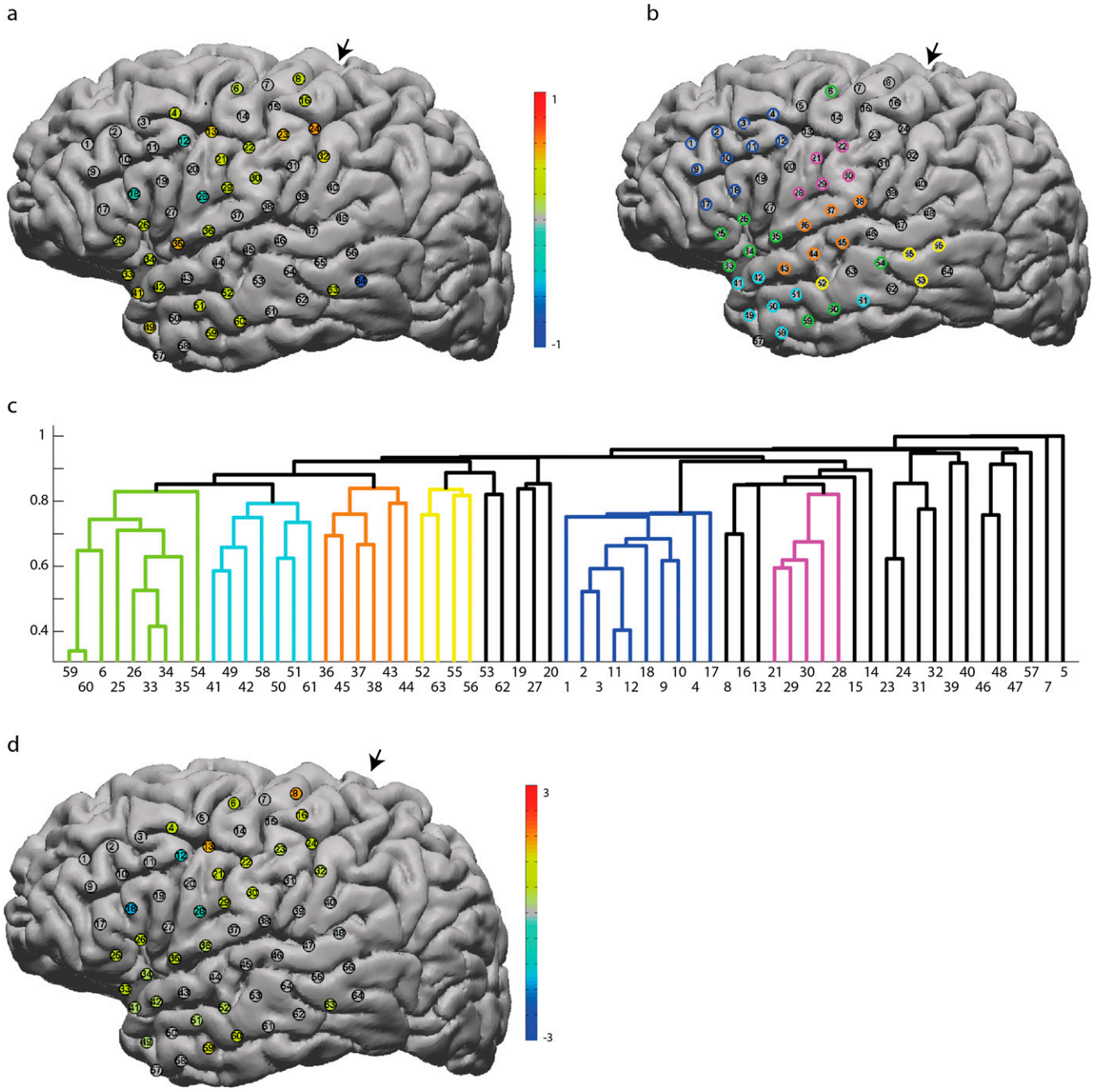

Fig. S4. Subject 4 results (control). (*A*) For each electrode, the difference between the average rate of spindle occurrence in pre- and posttraining sleep is plotted on the subject's cortex as a ratio of the sum of the means. Warm colors indicate a rate increase; cool colors indicate a rate decrease. Electrodes that showed no significant ($P < 0.001$, Bonferroni corrected for multiple comparisons) change are drawn in gray. This is a control subject so there is no task electrode. (*B*) Coincidence-based "distance" was used to cluster electrodes in spindle space. The dendrogram (*C*) shows the relative closeness of electrodes in this space. In this case, the dendrogram was created from posttraining sleep. The distance between electrodes, plotted on the *x* axis, has a maximum value of 1 and a minimum value of 0. Clusters are formed by setting a distance threshold; here a threshold of 85% of the maximum distance was used. Example clusters are shown in different colors in the dendrogram and plotted with the same colors on the cortex (*B*). (*D*) The absolute difference between the average rate of spindle occurrence in pre- and posttraining sleep is plotted on the subject's cortex. Warm colors indicate a rate increase; cool colors indicate a rate decrease. Electrodes that showed no significant ($P < 0.001$, Bonferroni corrected for multiple comparisons) change are drawn in gray. The central sulcus is marked with a black arrow in *A*–*D*.

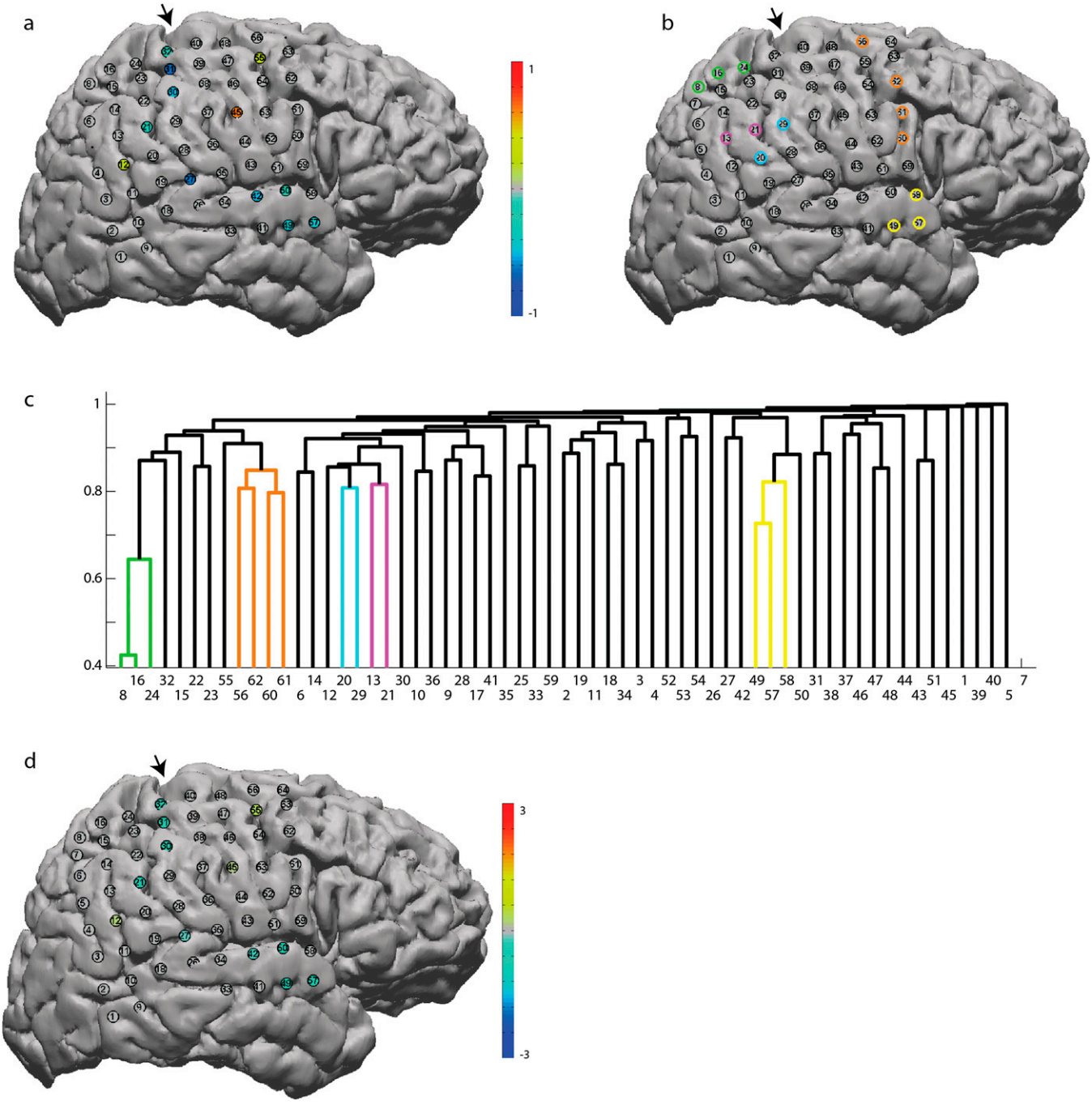

Fig. S5. Subject 5 results (control). (*A*) For each electrode, the difference between the average rate of spindle occurrence in pre- and posttraining sleep is plotted on the subject's cortex as a ratio of the sum of the means. Warm colors indicate a rate increase; cool colors indicate a rate decrease. Electrodes that showed no significant ($P < 0.001$, Bonferroni corrected for multiple comparisons) change are drawn in gray. This is a control subject so there is no task electrode. (*B*) Coincidence-based "distance" was used to cluster electrodes in spindle space. The dendrogram (*C*) shows the relative closeness of electrodes in this space. In this case, the dendrogram was created from posttraining sleep. The distance between electrodes, plotted on the *x* axis, has a maximum value of 1 and a minimum value of 0. Clusters are formed by setting a distance threshold; here a threshold of 85% of the maximum distance was used. Example clusters are shown in different colors in the dendrogram and plotted with the same colors on the cortex (*B*). (*D*) The absolute difference between the average rate of spindle occurrence in pre- and posttraining sleep is plotted on the subject's cortex. Warm colors indicate a rate increase; cool colors indicate a rate decrease. Electrodes that showed no significant ($P < 0.001$, Bonferroni corrected for multiple comparisons) change are drawn in gray. The central sulcus is marked with a black arrow in *A*–*D*.

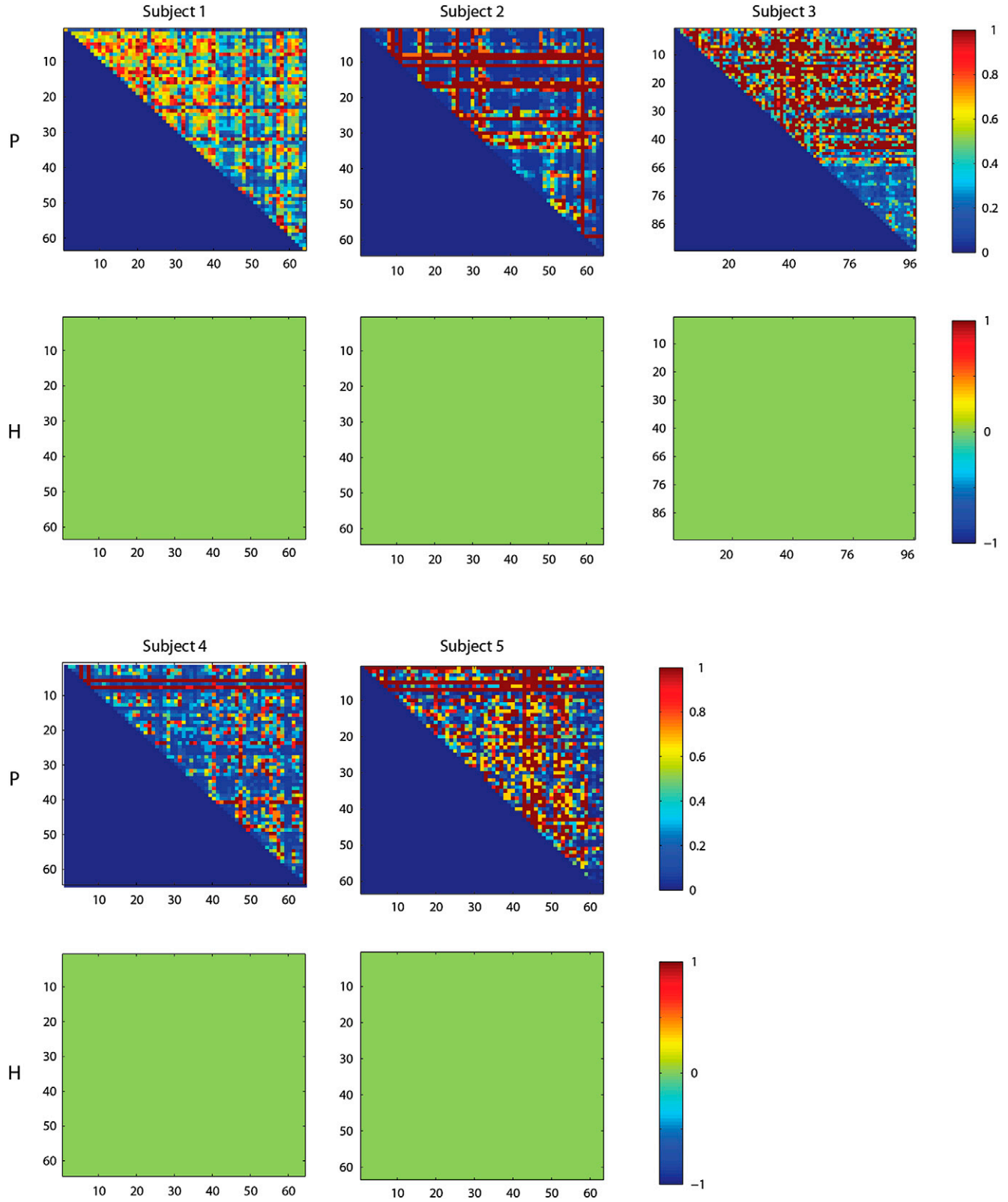

Fig. S6. Coincidence matrix statistics. For each subject, the similarity of the coincidence matrices for days 1 and 2 were evaluated. For each electrode pair, a rank sum test was performed to determine whether the medians of pre- and posttraining coincidence were significantly different at a *P* value of 0.05 (Bonferroni corrected for multiple comparisons). For each subject, (*Upper*) *P* value matrix. (*Lower*) Significance (H) matrix. The coincidence was not significantly different between the two nights for any electrode pair.